USCAP

ARTICLE

# Pharmacological inhibition of serine synthesis enhances temozolomide efficacy by decreasing $O^6$-methylguanine DNA methyltransferase (MGMT) expression and reactive oxygen species (ROS)-mediated DNA damage in glioblastoma

Lei Jin[1], Karrie Mei-Yee Kiang[1], Stephen Yin Cheng[1] and Gilberto Ka-Kit Leung[1]✉



Glioblastoma (GBM) is the most malignant primary tumor in the central nervous system of adults. Temozolomide (TMZ), an alkylating agent, is the first-line chemotherapeutic agent for GBM patients. However, its efficacy is often limited by innate or acquired chemoresistance. Cancer cells can rewire their metabolic programming to support rapid growth and sustain cell survival against chemotherapies. An example is the de novo serine synthesis pathway (SSP), one of the main branches from glycolysis that is highly activated in multiple cancers in promoting cancer progression and inducing chemotherapy resistance. However, the roles of SSP in TMZ therapy for GBM patients remain unexplored. In this study, we employed NCT503, a highly selective inhibitor of phosphoglycerate dehydrogenase (PHGDH, the first rate-limiting enzyme of SSP), to study whether inhibition of SSP may enhance TMZ efficacy in MGMT-positive GBMs. 3-(4,5-dimethylthiazol-2-yl)-2,5-diphenyltetrazolium bromide (MTT), flowcytometry and colony formation assays demonstrated that NCT503 worked synergistically with TMZ in suppressing GBM cell growth and inducing apoptosis in T98G and U118 cells in vitro. U118 and patient-derived GBM subcutaneous xenograft models showed that combined NCT503 and TMZ treatment inhibited GBM growth and promoted apoptosis more significantly than would each treatment alone in vivo. Mechanistically, we found that NCT503 treatment decreased MGMT expression possibly by modulating the Wnt/β-catenin pathway. Moreover, intracellular levels of reactive oxygen species were elevated especially when NCT503 and TMZ treatments were combined, and the synergistic effects could be partially negated by NAC, a classic scavenger of reactive oxygen species. Taken together, these results suggest that NCT503 may be a promising agent for augmenting TMZ efficacy in the treatment of GBM, especially in TMZ-resistant GBMs with high expression of MGMT.

*Laboratory Investigation* (2022) 102:194–203; https://doi.org/10.1038/s41374-021-00666-7

## INTRODUCTION

Glioblastoma multiforme (GBM) is the most common malignant primary brain tumor in the central nervous system in adults[1]. Currently, the primary treatment option for GBM is maximal surgical resection followed by adjuvant chemotherapy and/or ionizing radiotherapy (Stupp's regimen)[2,3]. Although great research advances have been achieved in these treatment modalities over the past decades, the prognosis of GBM patients remains poor with a median survival of 12–15 months[3]. Rapid disease recurrence and treatment resistance are the two main obstacles to optimal patient outcomes[3]. Therefore, a better understanding of treatment resistance mechanisms and improving treatment efficacies are urgently needed.

Temozolomide (TMZ), an orally bioavailable alkylating agent featured with convenient route of administration, ready penetration across the blood brain barrier, tolerable safety profile and manageable side effects, is the Food and Drug Administration-approved first-line adjuvant chemotherapeutic agent for newly diagnosed GBMs since 1999 that had significantly improved GBM patients' survival[4]. TMZ exerts its antitumor effects by intermediate metabolites which can transfer methyl groups to guanine residues of DNA and trigger DNA damage and subsequent cell death[5]. However, the clinical therapeutic value of TMZ is limited due to innate or adaptive resistance[6]. $O^6$-methylguanine DNA methyltransferase (MGMT), a DNA repair protein, is able to remove the methyl adducts from the $O^6$ position of guanine residues and therefore mediates the TMZ resistance in glioma cells[7]. MGMT expression is controlled by epigenetic modifications: methylation and high methylation in the promoter region may decrease gene transcription and subsequent protein translation of MGMT[8]. Clinical studies have also revealed that GBM patients bearing the absence of MGMT protein or high methylation of the MGMT promoter would benefit more from TMZ treatment[9–11], indicating that high MGMT expression remains a main cause for poor TMZ-related chemotherapy efficacy in GBM. Therefore, inhibition of MGMT expression holds marked potential for counteracting TMZ resistance.

[1]Department of Surgery, Li Ka Shing Faculty of Medicine, the University of Hong Kong, Hong Kong, China. ✉email: gilberto@hku.hk

Received: 13 July 2021 Revised: 12 August 2021 Accepted: 12 August 2021
Published online: 8 October 2021

Compared to normal cells, malignant tumor cells can rewire metabolic programming to increased glycolysis regardless of oxygen availability to produce macromolecules to support rapid growth and antioxidants to defy oxidative stress, i.e., the "Warburg Effect"[12]. It is reasonable to speculate that rewired tumor metabolism may also affect the response of tumor cells to chemotherapeutic agents, and targeting specific metabolic pathways and/or key enzymes may be potential strategies to enhance chemotherapeutic efficacy[13]. De novo serine biosynthesis pathway branches off from glycolysis and diverts the glycolytic intermediate 3-phosphoglycerate to 3-phosphohydroxypyruvate to support energy demand, cellular redox balance and one carbon biosynthesis[12]. This pathway has been reported to be highly activated and condusive to tumor progression in multiple types of cancers such as breast cancer[14], lung cancer[15,16], and glioblastoma[17]. Several research groups also demonstrated that genetic or pharmacological inhibition of phosphoglycerate dehydrogenase (PHGDH), a key rate-limiting enzyme of the serine synthesis pathway, could enhance chemotherapy efficacy or even reverse chemoresistance in malignant tumors including hepatocellular carcinoma[18], lung cancer[19], melanoma[20], and Burkitt lymphoma[21]. However, the roles of PHGDH in TMZ resistance in GBM remain unknown.

Herein, we explored whether and how inhibition of PHGDH with a highly selective inhibitor NCT503 could enhance TMZ chemoefficacy in GBM in vitro and in vivo. We show that NCT503 works synergistically with TMZ in suppressing GBM growth and inducing apoptosis both in vitro and in vivo. Mechanistically, NCT503 treatment inhibits MGMT expression possibly by modulating the Wnt/β-catenin pathway and augmenting reactive oxygen species (ROS)-mediated DNA damage.

## MATERIAL AND METHODS

### Cell lines and cell culture

U87, U251, D54, A172, LN229, T98G, and U118 glioblastoma cell lines were purchased from the American Type Culture Collection (ATCC, Manasaas, VA, USA). U87 and U251 cells were cultured in Minimum Essential Medium α. D54 cells were cultured in Dulbecco's Modified Eagle's Medium/Nutrient Mixture F-12 supplemented with glutamine (GlutaMAX$^{TM}$-I). A172, LN229, T98G and U118 cells were cultured in DMEM. All these media were commercially available from ThermoFisher (Waltham, MO, USA) and supplemented with 10% fetal bovine serum (Gibco) and 1% penicillin/streptomycin for cell culture at 37 °C in an incubator containing 5% $CO_2$ under saturated humidity.

### Antibodies and reagents

Mouse primary anti-MGMT antibody (sc-56432) was commercially available from Santa Cruz (Dallas, TX, USA). Rabbit primary anti-LEF1 (A4473) and anti-TCF1/7 (A3091) were from ABclonal (Woburn, MA, USA). Other primary antibodies including PARP (9532T), Cleaved Caspase 3 (9661S), Bax (5023T), Bcl-2 (4223T), β-catenin (8480T), c-Myc (18583T), Cyclin D1 (2936T), p-H2A.X (9718T), and GAPDH (5174S) were all purchased from Cell Signaling (CST, MA, USA). The PHGDH inhibitor NCT503 (HY101966), Tween-80 (HY-Y1891), and polyethylene glycol 400 (PEG400) (HY-Y0873A) were purchased from MedChemExpress (MCE, Monmouth Junction, NJ, USA) while dimethyl sulfoxide (DMSO) (C6164) and N-Acetyl cysteine (NAC) (A0737) were from Sigma-Aldrich (St. Louis, MO, USA). TMZ was obtained from Schering-Plough (Kenilworth, NJ, USA), dissolved in DMSO at a concentration of 100 mM, further diluted to 10 mM in culture medium and stored at −20 °C.

### Flowcytometry apoptosis assay

Apoptosis assay was performed with an apoptosis detection kit (Roche, Basel, Switzerland) according to the manufacturer's instructions. After drug treatment, the medium was discarded and the cells were washed with 1× PBS and trypsinized with EDTA-free trypsin. Single cells were then collected, washed with 1× PBS for two times and incubated with propidium iodide (PI) and annexin V for 15 min at room temperature in the dark. Cells were then filtered with 40 μm cell strainer and subject to flowcytometry analysis using the CytoFLEX S Flow Cytometer (Beckman Coulter, Indianapolis, IN, USA). The percentage of annexin V-positive cells was acquired and subject to statistical analysis.

### Cell viability assay

T98G or U118 cells were collected and seeded at 3000 cells/well in 96-well plates. Following drug treatments at designated time points, the medium was discarded and the cells were washed with PBS once. Fresh complete medium (90 μL) supplemented with 10 μL of 3-(4,5-dimethylthiazol-2-yl)-2,5-diphenyltetrazolium bromide (MTT) (Sigma-Aldrigh) was then added to incubate the cells for 3 h. After discarding the medium, MTT was then dissolved in DMSO (100 μL) for 15 min on a shaker and the absorbance was assessed by measuring the optical density at 570 nm using a microplate reader (Thermo Fisher Scientific).

### Colony formation assay

T98G or U118 cells were collected and seeded at 600 cells/well in 6-well plates. After treatment with NCT503 alone or in combination with temozolomide or NAC for 48 or 72 h, the medium was replaced with 2 mL of fresh medium and the cells were further cultured for 10–14 days. Colonies were stained with 0.5% crystal violet, and the numbers of colonies were counted and subject to statistical analysis.

### Protein extraction and western blot

Total protein was extracted from fresh tumor sample or cultured cells with 1× RIPA lysis buffer (Cell Signaling, MA, USA) supplemented with cocktail protease inhibitor (Roche, Risch-Rotkreuz, Switzerland). Protein concentrations were determined using protein assay reagents (Bio-Rad Laboratories, Herclues, CA, USA) according to the manufacturer's instructions. Twenty migrogram of each protein sample was then subject to 10% sodium dodecyl sulfate-polyacrylamide gel electrophoresis gel electrophoresis and transferred to polyvinylidene difluoride membrane (Millipore). Membranes were blocked with 5% nan-fat milk for 1 h at room temperature and then incubated with primary antibodies all at appropriate dilutions at 4 °C overnight. GAPDH was used as loading control. Next day, horseradish peroxidase-conjugated goat anti-rabbit/mouse immunoglobulin G (1:5000) were used to incubate the membranes at room temperature for 1 h. After washing with 1× Tris buffered saline with Tween 20 (TBST), immunoblots were developed by enhanced chemiluminescence detection system with X-ray film in dark room. Band densities were quantified by Image J software (Image J 1.43u; National Institute of Health, Bethesda, MD, USA). The relative protein levels were determined by normalizing the densitometry values of protein of interest to that of GAPDH.

### DNA extraction, bisulfite treatment, and methylation-specific polymerase chain reaction (MS-PCR)

Genomic DNA was extracted from T98G or U118 cells after 0.1% DMSO or NCT503 (50 μM) treatment for 48 h using the Purelink™ Genomic DNA Mini Kit (K182001, Thermo Fisher Scientific) according to the manufacturer's instructions. The DNA quality was measured using Nanodrop 2000 (Thermo Fisher Scientific). Genomic DNA (500 ng) was bisulfite-treated using the EpiJET Bisulfite Conversion Kit (K1461, Thermo Fisher Scientific) according to the manufacturer's instructions to convert all unmethylated cytosine to uracil and leave the 5-methylcytosine unaltered. Converted DNA (2 μL) was subject to MS-PCR using 2 primer pairs designed for the amplification of the methylated and unmethylated alleles of the *MGMT* promoter. The primer sequences for unmethylated reactions were 5′-TTTGTGTTTTGATGTTTGTAGGTTTTTGT-3′ (forward) and 5′-AACTCCA-CACTCTTCCAAAAACAAAA-3′ (reverse) while those for methylated reactions were 5′-TTTCGACGTTCGTAGGTTTTCGC-3′ (forward) and 5′-GCACTCTTCCGAAAACGAAACG-3′ (reverse). PCR was performed in a SimpliAmp™ thermal cycler (Applied Biosystems, Waltham, MA, USA) and the PCR conditions were as follows: 95 °C 5 min; (95 °C 30 s, 59 °C 30 s, 72 °C 30 s) × 42 cycles; 72 °C 5 min. Twenty microliters of PCR products (30 μL in total) were loaded on 2% agarose gel and separated by electrophoresis. The gel was incubated with 0.5 μg/mL ethidium bromide for 15 min at room temperature and then visualized under ultraviolet illumination.

### Immunofluorescence staining (IF)

$5 \times 10^3$ T98G or U118 cells were firstly seeded in 96-well plates. After treatment with 50 μM NCT503 or 800 μM TMZ alone or in combination for 48 h, cells were washed with 1× PBS, fixed with 4% paraformaldehyde

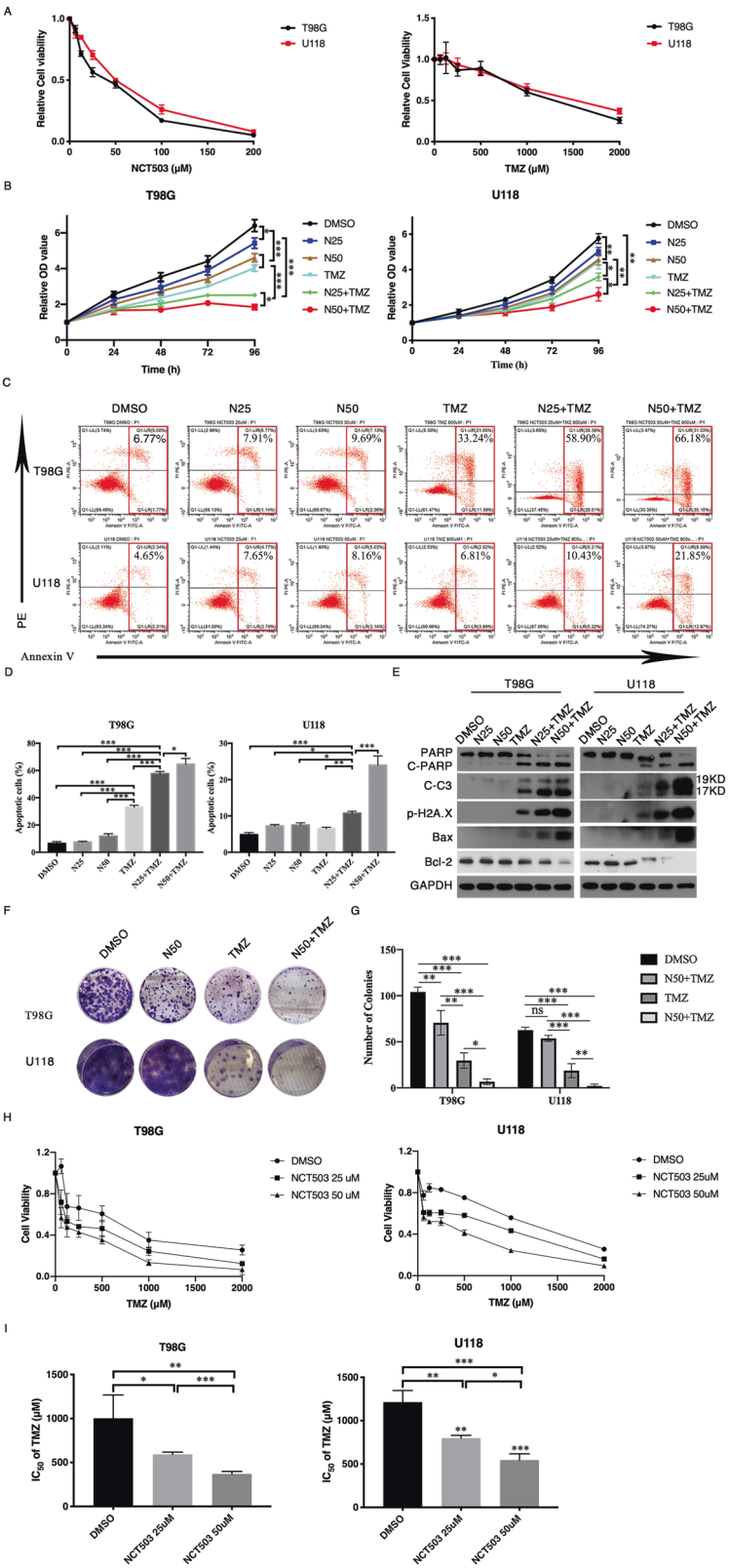


(PFA) and permeabilized with 0.5% Triton-X-100. 3% bovine serum albumin (BSA) was used for nonspecific blocking. Cells were then incubated with anti-MGMT primary antibody at a dilution of 1:50 in 1% BSA overnight at 4 °C. Next day, after three washes with 1X TBST, cells were incubated with mouse fluorescein-conjugated secondary antibody at a dilution of 1:500 in 1% BSA for 1 h at room temperature, followed by nuclear staining with Hoechst (1:100) for 1 h at room temperature. Immunofluorescence images were acquired under a fluorescent microscope (EVOS, Life Technologies).

## ROS measurement

Intracellular ROS levels were detected using the 2′-7′-dichlorodihydrofluorescein diacetate (DCFH-DA) Cellular ROS Detection Kit (ab113851, Abcam,

**Fig. 1 NCT503 augments TMZ-mediated chemotherapy in MGMT-positive GBM cells. A** MTT assay measured the toxic effects of a series of concentration of NCT503 (0, 6.25, 12.5, 25, 50, 100, and 200 μM) and TMZ (0, 62.5, 125, 250, 500, 1000, and 2000 μM) on T98G and U118 cells. **B** MTT assay measured the anti-proliferative effects of NCT503 or TMZ treatment alone or in combination on T98G and U118 cells at 0, 24, 48,72, and 96 h. N25: NCT503 25 μM; N50: NCT503 50 μM; TMZ: 1000 μM. **C**, **D** Flowcytometry apoptosis assay assessed the pro-apoptotic effects of NCT503 or TMZ treatment alone or in combination on T98G and U118 cells for 48 h. **E** Western blot detected the expression levels of apoptosis-related proteins including cleaved PARP (C-PARP), Cleaved Caspase 3 (C-C3), Bax, and Bcl-2. **F**, **G** Colony formation assay evaluated the effects of NCT503 or TMZ treatment alone or in combination on clonogenicity of T98G and U118 cells. **H**, **I** MTT assay measured the responses of T98G and U118 cells to different concentrations of TMZ (0, 62.5, 125, 250, 500, 1000, and 2000 μM) in the absence (DMSO) or presence of NCT503 (25 and 50 μM). *$P < 0.05$; **$P < 0.01$; ***$P < 0.001$.

Cambridge, UK) according to the manufacturer's protocol. Briefly, after drug treatment the cells were trypsinized, washed with 1× PBS for two times and then incubated with 10 μM DCFH-DA in PBS for 15 min at 37 °C. Stained cells were filtered and then analyzed by flowcytometry. Acquired data were analyzed by FlowJo Software (FlowJo).

### Xenograft model

One cell-derived subcutaneous xenograft model (U118) and one patient-derived subcutaneous glioblastoma xenograft (GBM#10 PDX) were included to study the combinatorial effects of TMZ and NCT503 on tumor growth according to previous reports. The authenticity of GBM#10 PDX was validated by short tandem repeat DNA sequencing (Supplementary file 1). Male athymic BALB/c nude mice or nonobese diabetic/severe combined deficiency (NOD SCID) mice aged 4–6 weeks and weighed ~20 g were obtained from the Laboratory Animal Unit of the University of Hong Kong for U118 or GBM#10 PDX xenograft model, respectively. For the establishment of U118 and GBM#10 PDX subcutaneous xenograft models, U118 cell suspension ($1 \times 10^6$) mixed with Matrigel (356234, Corning) at 1:1 in a total volume of 100 μL or small pieces of fresh GBM#10 tumor (50 $mm^3$) was implanted into the right flanks of mice. When the volume of subcutaneous xenografts reached 50 $mm^3$, mice were randomly divided into four groups: Vehicle, NCT503, TMZ and NCT503 + TMZ. Temozolomide in 1× PBS was oral-gavaged to the mice with Ora-Plus at 10 mg/kg/day every other day for 12 days while NCT503 in a vehicle containing 5% DMSO, 5% Tween-80 and 5% PEG-400 was injected intraperitoneally at 40 mg/kg/day for 12 consecutive days. Tumor volume was calculated and recorded routinely according to the formula: $V = ½ab^2$, with $a$ and $b$ representing the longest and shortest diameter. Tumor weight was also measured immediately after isolation at the end of treatment. Body weights of mice were recorded and subject to statistical analysis.

### Statistical analysis

In vitro experiments were repeated at least three times and the data were expressed as mean ± standard deviation. Comparisons between two groups were performed by student's $t$ test while differences among three or more groups were assessed by one-way analysis of variance followed by Tukey's multiple comparison test. Statistical analyses were performed using GraphPad Prism 7 (GraphPad Software, San Diego, CA) and SPSS version 13.0 (SPSS Inc, Chicago, IL). Tests were two-tailed and $P < 0.05$ was considered statistically significant.

## RESULTS

### NCT503 enhances temozolomide chemo-efficacy in MGMT-positive GBM cells

The MGMT expression levels in seven human GBM cell lines (U87, U251, D54, U118, T98G, A172, and LN229) and one human GBM PDX (GBM#10 PDX) were firstly detected with western blot. Consistent with previous reports[22], MGMT expression was present in T98G and U118 cell lines while the human GBM PDX showed present but relatively low MGMT protein expression when compared to in T98G and U118 cell lines (Supplementary Fig. 1). T98G and U118 cell lines were then selected for subsequent in vitro experiments. The cytotoxic effects of NCT503 and TMZ alone on human GBM cell lines T98G and U118 with MTT assay were assesed.

As shown in Fig. 1A, after NCT503 and TMZ treatment for 72 h, cell viabilities decreased in a concentration-dependent manner in both cell lines with the $IC_{50}$ of NCT503 being around 50 μM while that of TMZ being around 1000 μM. 25 and 50 μM of NCT503 and 1000 μM of TMZ were chosen for subsequent experiments. To test whether inhibition of PHGDH could work synergistically with TMZ, cells were treated with 0.1% DMSO, 25 μM NCT503, 50 μM NCT503, 1000 μM TMZ, and 25 μM or 50 μM NCT503 together with 1000 μM TMZ, respectively. Antiproliferative effects were measured with MTT assay and showed that NCT503 treatment alone inhibited cell growth in a concentration-dependent manner and 50 μM NCT503 treatment achieved similar inhibitory effect as 1000 μM TMZ in both cell lines. Notably, combination of NCT503 and TMZ dramatically reduced cell viabilities in both cell lines also in a dose-dependent manner compared with the NCT503 or TMZ treatment alone groups (Fig. 1B). Flowcytometry apoptosis assay was employed to evaluate the pro-apoptotic effects and demonstrated that NCT503 treatment alone induced slight but not significant apoptosis in T98G and U118 cells. TMZ treatment alone induced 33.24% apoptosis in T98G cells but insignificant apoptosis in U118 cells. Strikingly, when these two treatments were combined, apoptosis was remarkably elevated in a dose-dependent manner in both cell lines. For T98G cells, the percentage of apoptotic cells was increased to 58.90% and 66.18%, respectively after the addition of 25 μM or 50 μM NCT503 compared to TMZ treatment alone (33.24%). For U118 cells, the percentage of apoptotic cells was increased to 10.73% and 21.85%, respectively after the addition of NCT503 compared to TMZ treatment alone (6.53%) (Fig. 1C, D). This observation was validated by the expression levels of several well recognized apoptosis-related proteins including cleaved PARP, cleaved caspase 3, Bax, and Bcl-2 with western blot (Fig. 1E). Colony formation assay was also included and showed that NCT503 treatment alone reduced colony numbers in T98G cells but not in U118 cells while TMZ treatment alone significantly reduced colony numbers in both cell lines. Consistent with the MTT and flowcytometry apoptosis assay observations, combination of NCT503 and TMZ more significantly inhibited colony formation in both cell lines (Fig. 1F, G). To determine whether the addition of NCT503 could lower $IC_{50}$ of TMZ, T98G and U118 cells were treated with a series of concentrations of TMZ with or without of 25 or 50 μM NCT503 for 72 h. MTT assay demonstrated that supplementation of NCT503 treatment significantly reduced $IC_{50}$ of TMZ in a dose-dependent manner in both cell lines (Fig. 1H, I). These results suggest that NCT503 could enhance TMZ chemo-efficacy in vitro.

### NCT503 augments temozolomide chemo-efficacy in MGMT-positive GBM in vivo

To test whether NCT503 could also enhance TMZ efficacy in vivo, U118 subcutaneous xenograft model and GBM#10 PDX were employed and treated with NCT503 and/or TMZ alone for two weeks. In the U118 xenograft model, NCT503 alone or TMZ treatment alone showed slight inhibitory effects which were not statistically significant (vs NCT503, $P = 0.1722$; vs TMZ, $P = 0.2103$). But when used in combination, xenograft growth was significantly suppressed (vs Vehicle, $P < 0.001$; vs NCT503, $P = 0.0059$; vs TMZ, $P = 0.0045$) (Fig. 2A, C). Similarly in the GBM#10 PDX model, slight but insignificant inhibition of xenograft growth was observed with

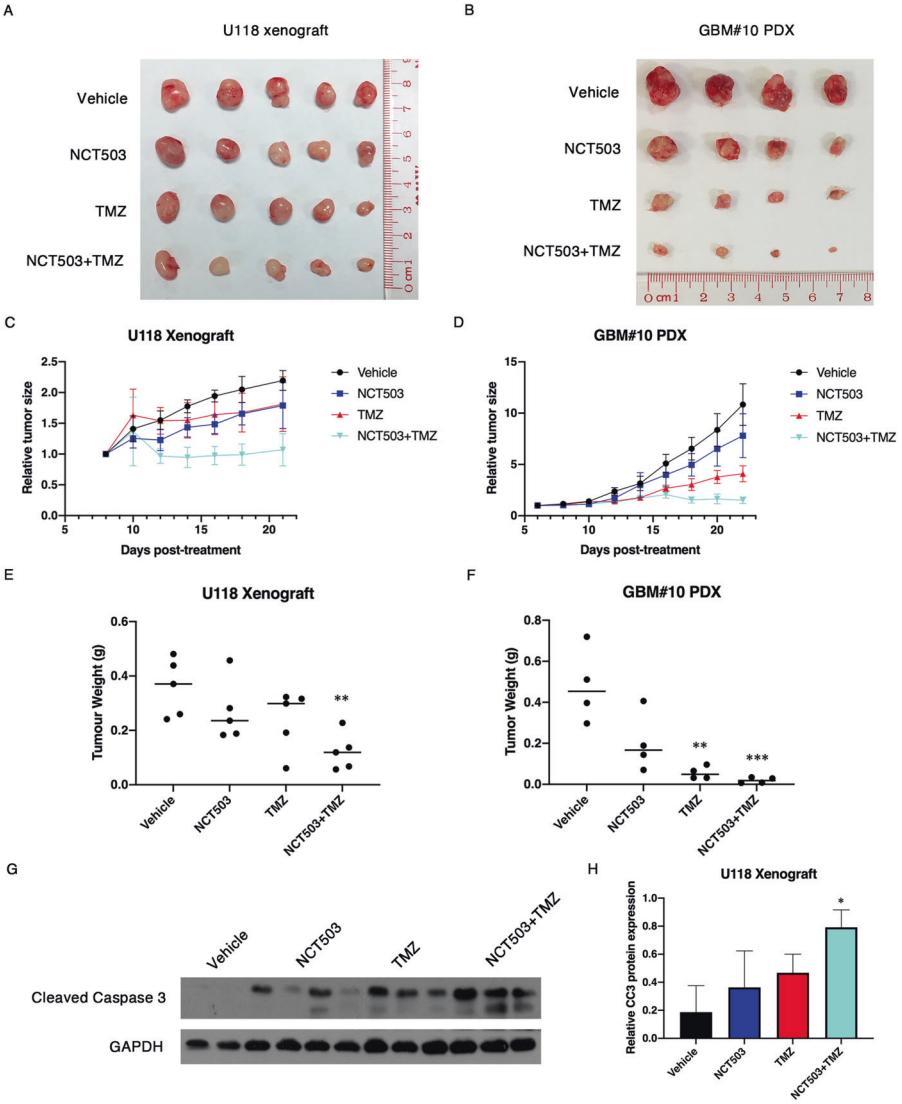


**Fig. 2 NCT503 enhances TMZ efficacy in vivo. A**, **B** Representative images of U118 and GBM#10 PDX subcutaneous xenografts after treatment with NCT503 or TMZ alone or in combination for 2 weeks. **C**, **D** Xenograft size was recorded every 2 days with a caliper and normalized to that on the day before treatment. Growth curves were plotted accordingly. **E**, **F** Xenograft weights were measured immediately after isolation and subject to one-way ANOVA analysis. **G**, **H** Western blot detected the protein expression levels of apoptosis marker: cleaved caspase 3. GAPDH was used as the internal control. Differences were analyzed by one-way ANOVA analysis. $*P < 0.05$; $**P < 0.01$; $***P < 0.001$.

NCT503 treatment alone ($P = 0.1064$). Of note, TMZ treatment significantly inhibited the xenograft growth ($P = 0.0022$). Strikingly, combination of NCT503 and TMZ treatment almost ceased xenograft growth (vs Vehicle, $P < 0.001$; vs NCT503, $P = 0.0011$; vs TMZ, $P = 0.0498$) (Fig. 2B, D).

Xenografts were then harvested for further assays. The NCT503 + TMZ group displayed the lowest tumor weights in both xenograft models (U118 xenograft, $P = 0.0369$; GBM#10 PDX, $P = 0.0005$) (Fig. 2E, F). Total protein from fresh U118 xenografts was extracted and subject to western blot. In the NCT503 + TMZ group, cleaved caspase 3 was significantly elevated ($P = 0.0219$) (Fig. 2G, H). Adverse effects of NCT503 and TMZ treatment were also evaluated. No significant decrease in body weight was observed in both xenograft models during the course of treatment (Supplementary Fig. 2A, B). H&E staining showed no obvious organ damages (Supplementary Fig. 2C). These results suggest that NCT503 could augment TMZ chemo-efficacy in vivo without causing adverse systemic side-effects.

## NCT503 inhibits MGMT expression in glioblastoma by modulating Wnt/β-catenin pathways

To examine how NCT503 contributed to TMZ chemo-efficacy, MGMT expression was firstly detected by western blot since the presence of MGMT in glioma cell lines such as T98G and U118 cells has been widely believed to be a major reason for TMZ resistance. As shown in Fig. 3A, B, MGMT protein levels remained almost unchanged when exposed to TMZ but was significantly reduced in the presence of NCT503 alone or in combination with TMZ in both T98G and U118 cells. This observation was further validated by immunofluorescence staining on T98G and U118 cells (Fig. 3C) and western blot with U118 xenografts after treatment with NCT503 and TMZ (Fig. 3D, E). A recent study in Burkitt lymphoma has reported that NCT503 treatment reduced serine production and global DNA and histone methylation[21]. Consistently, we found that NCT503 treatment reduced global methylation level in GBM cells in a dose-dependent manner evidenced by decreased H3 and H3K27M protein expressions (Supplementary Fig. 3A).

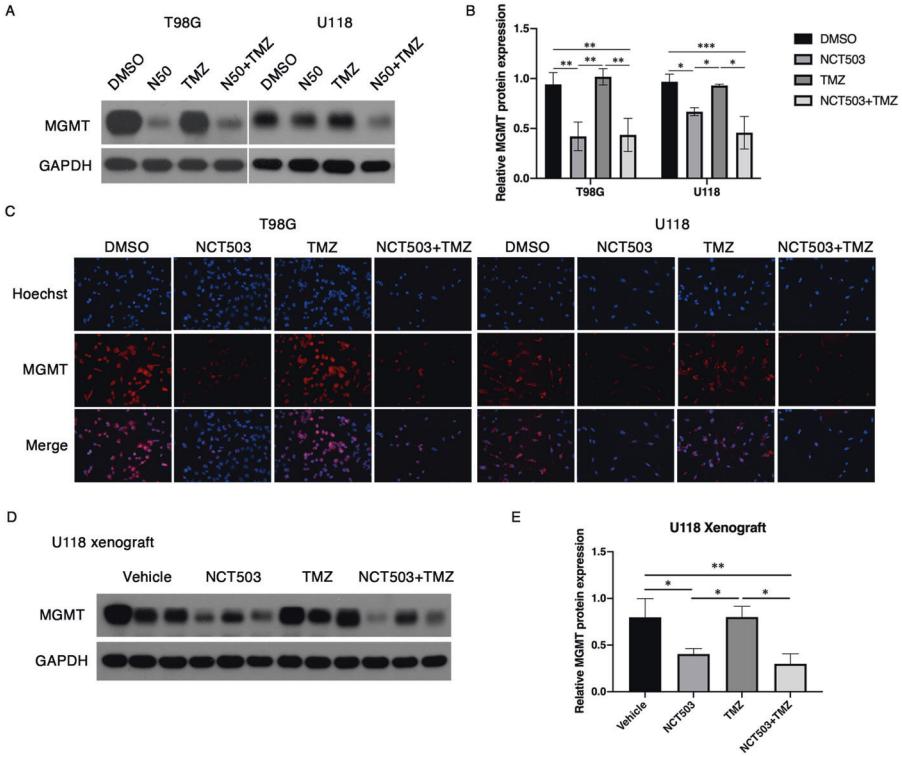


**Fig. 3 NCT503 inhibits MGMT expression in MGMT-positive GBM cells and xenografts. A**, **B** Western blot detected the protein expressions of MGMT in T98G and U118 cells after treatment with NCT503 or TMZ alone or in combination for 48 h. GAPDH was used as the loading control. N50: NCT503 50 μM. TMZ: 1000 μM. Differences were determined by one-way ANOVA analysis. **C** Immunofluorescence staining measured the expressions of MGMT in T98G and U118 cells after treatment with NCT503 (50 μM) or TMZ (1000 μM) alone or in combination for 48 h. **D**, **E** Western blot detected the protein expressions of MGMT in U118 subcutaneous xenografts after treatment with NCT503 (10 mg/kg/day) or TMZ (40 mg/kg/day) alone or in combination for 14 two weeks. $N = 3$ for each group. GAPDH was used as the loading control. Differences were determined by one-way ANOVA analysis. *$P < 0.05$; **$P < 0.01$; ***$P < 0.001$.

However, this contradicts the notion that decreased methylation on the promotor region of MGMT would increase the expression of MGMT. To clarify this, MS-PCR was performed and found that the *MGMT* promoter methylation level remained almost unchanged after NCT503 treatment in both T98G and U118 cell lines (Supplementary Fig. 3B). These results suggest the involvement of other regulatory mechanisms. Recent studies have shown that the Wnt/β-catenin pathway could be involved in regulating the expression of MGMT in cancers including GBM[23,24]. To determine whether NCT503-mediated MGMT decrease, as observed in this study, could be related to Wnt/β-catenin pathway, western blot was performed and showed that β-catenin protein expression was suppressed by NCT503 treatment in both T98G and U118 cells. In addition, two important downstream transcription factors LEF1 and TCF1/2 and two target genes c-Myc and Cyclin D1 also exhibited similar decreases to those of MGMT and β-catenin (Fig. 4A–C). These results suggest that NCT503 treatment may reduce MGMT expression through the Wnt/β-catenin pathway.

### NCT503 enhances TMZ efficacy partially via ROS-mediated DNA damage

In the meantime, emerging studies have reported that oxidative stress is also involved in chemotherapy resistance in many types of cancer including glioma[18]. The serine synthesis pathway provides de novo serine synthesis along with the production of nicotinamide adenine dinucleotide phosphate (NADPH), which is the major antioxidant in cells, suggesting that manipulation of this pathway might alter response of cancer cells to TMZ treatment. We measured the intracellular ROS levels using flowcytometry after the cells were treated with NCT503 and/or TMZ for 72 h and found that NCT503 treatment increased the ROS levels in both cell lines (T98G, $P < 0.001$; U118, $P = 0.0062$) while TMZ treatment increased the ROS levels in T98G cells ($P < 0.001$) but not in U118 cells ($P = 0.8824$). Notably, combination of NCT503 and TMZ significantly elevated the ROS levels in both cell lines compared to other groups (Fig. 5A). To determine whether increased ROS levels contributed to the synergistic inhibitory effects of NCT503 and TMZ, rescue assay was performed with the addition of 5 mM NAC, a classic ROS scavenger. As shown in Fig. 5B, MTT assay showed that NAC supplementation partially restored the cell viabilities decreased by NCT50-plus-TMZ treatment in T98G and U118 cells. Flowcytometry apoptosis assay demonstrated that addition of NAC in part lowered the percentage of apoptotic cells from 48.86% (NCT503 + TMZ) to 28.72% (NCT503 + TMZ + NAC) in T98G cells, and from 41.78% (NCT503 + TMZ) to 31.25% (NCT503 + TMZ + NAC) in U118 cells (Fig. 5C, D). This was further verified by western blot showing reduced cleaved PARP/PARP, cleaved caspase 3, Bax/Bcl-2, and the DNA damage marker, p-H2A.X (Fig. 5E). Colony formation assay showed that supplementation of NAC partially rescued the colony formation capacity in both cell lines (Fig. 5F, G). Finally, MTT assay was also included to assess whether NAC supplementation could restore the $IC_{50}$ of TMZ. As shown in Fig. 5H, I, $IC_{50}$ of TMZ was remarkably lowered to 655.0 μM and 669.2 μM in 98 G and U118 cell lines, respectively, when combined with 50 μM NCT503 while further supplementation of NAC partially restored $IC_{50}$ of TMZ to 846.3 μM and 886.5 μM, respectively. Taken together, these results suggest that NCT503 could enhance TMZ chemo-efficacy at least partially through ROS-induced DNA damages.

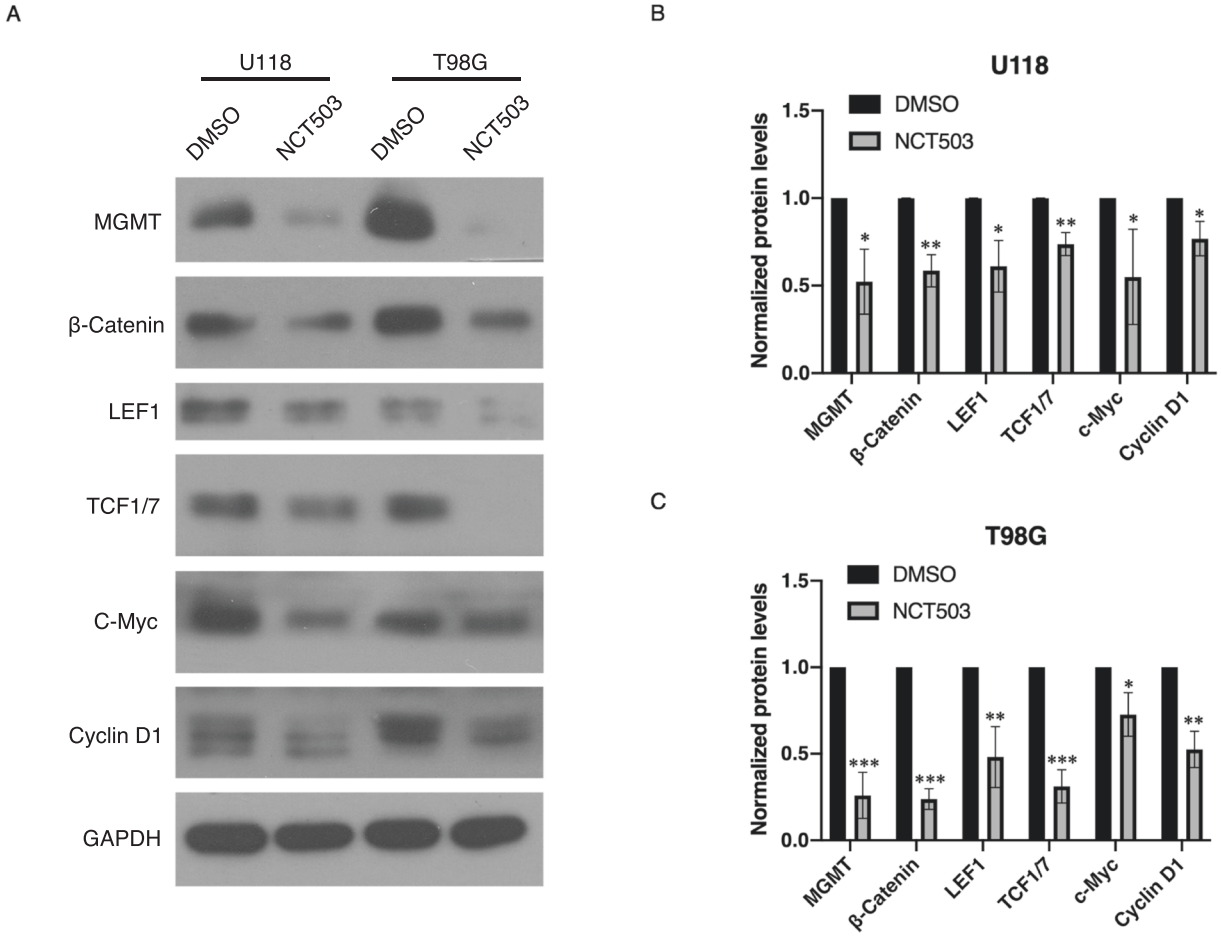


**Fig. 4 NCT503 inhibits Wnt/β-catenin pathway activity. A–C** Protein expression levels of β-catenin, two downstream transcriptional factors LEF1 and TCF1/7 and two target proteins c-Myc and Cyclin D1 were detected by western blot in T98G and U118 cells after treatment with 0.1% DMSO or NCT503 (50 μM) for 48 h and normalized to that of GAPDH for statistical analysis with student's t test. $^{*}P < 0.05$; $^{**}P < 0.01$; $^{***}P < 0.001$.

## DISCUSSION

TMZ is the first-line chemotherapeutic agent in GBM therapy. Given the extensive roles of de novo serine synthesis pathway in promoting tumor growth and inducing chemotherapy resistance in multiple cancers, we explored whether pharmacological inhibition of this way with a highly selective inhibitor NCT503 could enhance TMZ efficacy in GBM. We firstly showed that combination of NCT503 and TMZ treatment synergistically inhibited GBM cell growth, induced DNA damage and apoptosis, and reduced $IC_{50}$ of TMZ in a dose-dependent manner in vitro. Subcutaneous xenograft models also demonstrated that NCT503 and TMZ inhibited GBM growth more significantly when used in combination in vivo. Mechanistically, we found that NCT503 treatment enhanced TMZ efficacy by decreasing MGMT expression possibly through modulating Wnt/β-catenin pathway activity and ROS-mediated DNA damages.

Cancer cells demand various nutrients for the synthesis of biological macromolecules to support their proliferation and to sustain survival. Serine, a non-essential amino acid, provides precursors for the synthesis of nucleic acids, lipids and proteins essential for the growth of cancer cells[25]. Serine could be obtained from exogeneous uptake or endogenous biosynthesis by the de novo serine synthesis pathway, which consists of three rate-limiting enzymes: PHGDH, PSAT1 and PSPH[26]. The relationship between serine biosynthesis and cancer growth was first reported in liver cancer in a rat model[27]. In recent years, many studies have revealed that the SSP pathway is highly active in promoting tumor development and progression in multiple cancers[14–17,28–31]. Furthermore, studies have reported that combination of PHGDH inhibitors and chemotherapeutic drugs could enhance chemotherapy efficacy or even overcome chemotherapy resistance in breast cancer[32], myeloma[33], melanoma[20], lung adenocarcinoma[19], renal cell carcinoma[34], and hepatocellular carcinoma[18]. Consistent with these observations, our results showed that NCT503 treatment alone induce no significant DNA damage and apoptosis but a mild anti-proliferative effect in GBM cells. But when combined with TMZ, it caused more significant DNA damage and apoptosis and markedly lowered the $IC_{50}$ of TMZ in a dose-dependent manner in T98G and U118 cells. To our knowledge, our study is the first to demonstrate that NCT503 may serve as a chemosensitizer of TMZ in GBM therapy.

The presence of MGMT is one of the major causes for TMZ resistance in that it can remove the methyl adducts from the $O^6$ position of guanine residues and hinder TMZ-induced DNA damage and subsequent cell death[7]. Notably, methylation of the MGMT promoter has emerged as a strong prognostic factor in the therapy of GBM[9–11]. Thus, efforts to inhibit MGMT expression holds the potential to enhance TMZ efficacy in MGMT-positive GBMs. Serine biosynthesis pathway produces serine, which enters the folate cycle and provides one- carbon for epigenetic modification including methylation. It has been speculated that inhibition of this pathway might lower the global methylation status and increase the expression of MGMT in GBM. Indeed, we found that H3 and H3K27M both showed a concentration-dependent decrease after NCT503 treatment in T98G and U118 cells. However, MGMT protein expression levels displayed

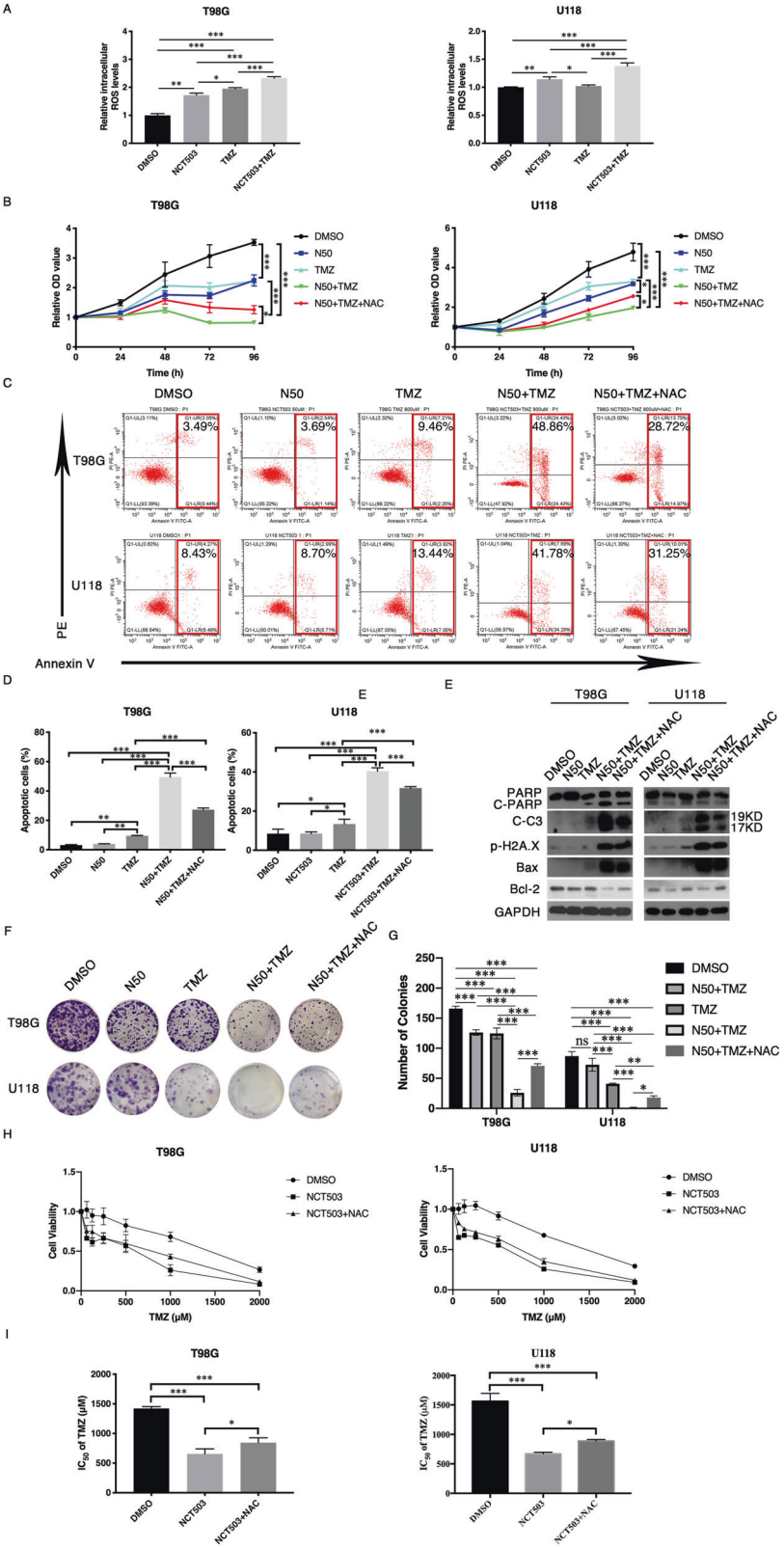


an entirely opposite trend. This contradiction drove us to measure the promotor methylation level of *MGMT* and found that it remained unchanged after NCT503 treatment, suggesting the involvement of other regulatory mechanisms. Wnt/β-catenin pathway plays a critical role in the development, progression and even recurrence of multiple malignant cancers[35–38]. Interestingly, this pathway has recently been reported to be also involved in the regulation of MGMT expression in several cancers including GBM[23,39–41]. Our results revealed that the activity of Wnt/β-catenin pathway was significantly suppressed upon NCT503 treatment, evidenced by the decrease in the protein

**Fig. 5 NCT503 augments TMZ efficacy partially by ROS-mediated DNA damage in MGMT-positive GBM cells. A** Flowcytometry detected the intracellular ROS levels after NCT503 (50 μM) or TMZ (1000 μM) treatment alone or in combination in T98G and U118 cells. **B** MTT assay measured the anti-proliferative effects of NCT503 or TMZ treatment alone or in combination with or without NAC (5 μM) supplementation on T98G and U118 cells at 0, 24, 48,72, and 96 h. N50: NCT503 50 μM. **C**, **D** Flowcytometry apoptosis assay assessed the pro-apoptotic effects of NCT503 or TMZ treatment alone or in combination with or without NAC supplementation on T98G and U118 cells for 48 h. **E** Western blot detected the expression levels of apoptosis-related proteins including cleaved PARP (C-PARP), Cleaved Caspase 3 (C-C3), Bax, Bcl-2, and p-H2A. X. **F**, **G** Colony formation assay evaluated the effects of NCT503 or TMZ treatment alone or in combination with or without NAC supplementation on clonogenicity of T98G and U118 cells. **H**, **I** MTT assay measured the responses of T98G and U118 cells to different concentrations of TMZ (0, 62.5, 125, 250, 500, 1000, and 2000 μM) in the absence (DMSO) or presence of NCT503 (50 μM) with or without NAC (5 μM) supplementation. $^{*}P < 0.05$; $^{**}P < 0.01$; $^{***}P < 0.001$.

expression levels of β-catenin, two important downstream transcription factors LEF1 and TCF1/7, and two target genes c-Myc and Cyclin D1, suggesting a possible association between NCT503 treatment and Wnt/β-catenin pathway. To our knowledge, we have revealed for the first time that NCT503 may inhibit MGMT expression by modulating the Wnt/β-catenin pathway. However, the exact regulatory mechanism between PHGDH and Wnt/β-catenin requires further investigation.

DNA damage and repair can be affected by cell metabolism in that the regulation of ROS through different metabolic pathways can increase oxidative damage to DNA[42]. For instance, NADPH, a major antioxidant, is produced when serine is neosynthesized, with around 40% of total NADPH being generated by the folate cycle with the conversion of serine into glycine[43]. What is more, nuclear factor erythroid 2-related factor 2 and glutathione have been reported to be key chemoresistance mediators with respect to TMZ in GBM[44]. These findings inspired us to speculate that NCT503 may be involved in TMZ-resistance by modulating oxidative stress. As expected, our results showed that NCT503 treatment increased the intracellular ROS levels especially when combined with TMZ, and NAC supplementation partially rescued the effects induced by NCT503 and TMZ. This is, to a certain extent, consistent with the observation that NCT503 treatment conferred oxidative disadvantage in several cancers such as hepatocellular carcinoma[18], lung cancer[19], and melanoma[20].

A few limitations of our study have to be mentioned here. For the in vivo experiments, we were unable to establish the intracranial MGMT-positive xenograft models using either the T98G and U118 cell lines even with the help of Matrigel as reported[45] and only the subcutaneous U118 and GBM#10 patient-derived subcutaneous xenograft models were included in the study. Since subcutaneous xenograft model may not reflect well the brain microenvironment[46], further validation of our finding with MGMT-positive intracranial models is required. Besides, the cell lines and xenograft models included in this study were all MGMT-positive. Whether NCT503 still enhances TMZ efficacy in MGMT-negative models with acquired resistance to TMZ remains unknown and needs further investigation.

In conclusion, our results demonstrate that pharmacological inhibition of PHGDH, a serine synthesis pathway enzyme, with NCT503 could synergistically work with TMZ in suppressing GBM growth and inducing apoptosis via decreasing MGMT expression possibly through interference with the Wnt/β-catenin pathway and ROS-mediated DNA damage. Combinational administration of NCT503 and TMZ may represent a novel and promising treatment strategy to enhance TMZ efficacy in patients with MGMT-high GBM.

## DATA AVAILABILITY

The datasets used during the current study are available from the corresponding author on reasonable request.

## REFERENCES

1. Lapointe, S., Perry, A. & Butowski, N. A. Primary brain tumours in adults. *Lancet* **392**, 432–446 (2018).
2. Stupp, R. et al. Radiotherapy plus concomitant and adjuvant temozolomide for glioblastoma. *N. Engl. J. Med.* **352**, 987–996 (2005).
3. Wen, P. Y. et al. Glioblastoma in adults: a Society for Neuro-Oncology (SNO) and European Society of Neuro-Oncology (EANO) consensus review on current management and future directions. *Neuro Oncol.* **22**, 1073–1113 (2020).
4. Stupp, R., Brada, M., van den Bent, M. J., Ton, J. C. & Pentheroudakis, G. High-grade glioma: ESMO Clinical Practice Guidelines for diagnosis, treatment and follow-up. *Ann. Oncol.* **25**, iii93–iii101 (2014).
5. Christmann, M., Verbeek, B., Roos, W. P. & Kaina, B. O(6)-Methylguanine-DNA methyltransferase (MGMT) in normal tissues and tumors: enzyme activity, promoter methylation and immunohistochemistry. *Biochim. Biophys. Acta* **1816**, 179–190 (2011).
6. Lee, S. Y. Temozolomide resistance in glioblastoma multiforme. *Genes Dis.* **3**, 198–210 (2016).
7. Hegi, M. E. et al. MGMT gene silencing and benefit from temozolomide in glioblastoma. *N. Engl. J. Med.* **352**, 997–1003 (2005).
8. Christmann, M. et al. MGMT activity, promoter methylation and immunohistochemistry of pretreatment and recurrent malignant gliomas: a comparative study on astrocytoma and glioblastoma. *Int. J. Cancer* **127**, 2106–2118 (2010).
9. Liu, G. et al. Analysis of gene expression and chemoresistance of CD133+ cancer stem cells in glioblastoma. *Mol. Cancer* **5**, 67 (2006).
10. van Nifterik, K. A. et al. Absence of the MGMT protein as well as methylation of the MGMT promoter predict the sensitivity for temozolomide. *Br. J. Cancer* **103**, 29–35 (2010).
11. Esteller, M. et al. Inactivation of the DNA-repair gene MGMT and the clinical response of gliomas to alkylating agents. *N. Engl. J. Med.* **343**, 1350–1354 (2000).
12. Liberti, M. V. & Locasale, J. W. The Warburg effect: how does it benefit cancer cells? *Trends Biochem. Sci.* **41**, 211–218 (2016).
13. Icard, P. et al. How the Warburg effect supports aggressiveness and drug resistance of cancer cells? *Drug Resist. Update* **38**, 1–11 (2018).
14. Pacold, M. E. et al. A PHGDH inhibitor reveals coordination of serine synthesis and one-carbon unit fate. *Nat. Chem. Biol.* **12**, 452–458 (2016).
15. Zhang, B. X. et al. PHGDH defines a metabolic subtype in lung adenocarcinomas with poor prognosis. *Cell Rep* **19**, 2289–2303 (2017).
16. Zhu, J. et al. High expression of PHGDH predicts poor prognosis in non-small cell lung cancer. *Transl. Oncol.* **9**, 592–599 (2016).
17. Liu, J. et al. Phosphoglycerate dehydrogenase induces glioma cells proliferation and invasion by stabilizing forkhead box M1. *J. Neurooncol.* **111**, 245–255 (2013).
18. Wei, L. et al. Genome-wide CRISPR/Cas9 library screening identified PHGDH as a critical driver for Sorafenib resistance in HCC. *Nat. Commun.* **10**, 4681 (2019).
19. Dong, J. K. et al. Overcoming erlotinib resistance in EGFR mutation-positive lung adenocarcinomas through repression of phosphoglycerate dehydrogenase. *Theranostics* **8**, 1808–1823 (2018).
20. Nguyen, M. Q. et al. Targeting PHGDH upregulation reduces glutathione levels and resensitizes resistant NRAS-mutant melanoma to MAPK kinase inhibition. *J. Invest. Dermatol.* **140**, 2242–2252 e2247 (2020).
21. Bialopiotrowicz, E. et al. Serine biosynthesis pathway supports MYC-miR-494-EZH2 feed-forward circuit necessary to maintain metabolic and epigenetic reprogramming of Burkitt lymphoma cells. *Cancers* **12**, 580 (2020).
22. Aasland, D. et al. Repair gene O-6-methylguanine-DNA methyltransferase is controlled by SP1 and up-regulated by glucocorticoids, but not by temozolomide and radiation. *J. Neurochem.* **144**, 139–151 (2018).
23. Wickstrom, M. et al. Wnt/beta-catenin pathway regulates MGMT gene expression in cancer and inhibition of Wnt signalling prevents chemoresistance. *Nat. Commun.* **6**, 8904 (2015).
24. Li, Z. Y. et al. Tanshinone IIA induces apoptosis via inhibition of Wnt/betacatenin/MGMT signaling in AtT20 cells. *Mol. Med. Rep.* **16**, 5908–5914 (2017).
25. Lukas, J., Lukas, C. & Bartek, J. More than just a focus: the chromatin response to DNA damage and its role in genome integrity maintenance. *Nat. Cell Biol.* **13**, 1161–1169 (2011).
26. Li, A. M. & Ye, J. B. The PHGDH enigma: do cancer cells only need serine or also a redox modulator? *Cancer Lett.* **476**, 97–105 (2020).

27. Davis, J. L., Fallon, H. J. & Morris, H. P. Two enzymes of serine metabolism in rat liver and hepatomas. *Cancer Res.* **30**, 2917–2920 (1970).
28. Chen, J. Y. et al. Phosphoglycerate dehydrogenase is dispensable for breast tumor maintenance and growth. *Oncotarget* **4**, 2502–2511 (2013).
29. Jing, Z. et al. Downregulation of phosphoglycerate dehydrogenase inhibits proliferation and enhances cisplatin sensitivity in cervical adenocarcinoma cells by regulating Bcl-2 and caspase-3. *Cancer Biol. Ther.* **16**, 541–548 (2015).
30. Jia, X. Q. et al. Increased expression of PHGDH and prognostic significance in colorectal cancer. *Transl. Oncol.* **9**, 191–196 (2016).
31. Xian, Y. et al. Phosphoglycerate dehydrogenase is a novel predictor for poor prognosis in gastric cancer. *Oncotargets Ther.* **9**, 5553–5560 (2016).
32. Zhang, X. & Bai, W. J. Repression of phosphoglycerate dehydrogenase sensitizes triple-negative breast cancer to doxorubicin. *Cancer Chemoth. Pharm.* **78**, 655–659 (2016).
33. Zaal, E. A. et al. Bortezomib resistance in multiple myeloma is associated with increased serine synthesis. *Cancer Metab.* **5**, 7 (2017).
34. Yoshino, H. et al. PHGDH as a key enzyme for serine biosynthesis in HIF2 alpha-targeting therapy for renal cell carcinoma. *Cancer Res.* **77**, 6321–6329 (2017).
35. Flahaut, M. et al. The Wnt receptor FZD1 mediates chemoresistance in neuroblastoma through activation of the Wnt/beta-catenin pathway. *Oncogene* **28**, 2245–2256 (2009).
36. Zhang, Z. M. et al. Pygo2 activates MDR1 expression and mediates chemoresistance in breast cancer via the Wnt/beta-catenin pathway. *Oncogene* **35**, 4787–4797 (2016).
37. Han, P. et al. The lncRNA CRNDE promotes colorectal cancer cell proliferation and chemoresistance via miR-181a-5p-mediated regulation of Wnt/beta-catenin signaling. *Mol. Cancer* **16**, 9 (2017).
38. Liebelt, B. D. et al. Glioma stem cells: signaling, microenvironment, and therapy. *Stem Cells Int*. **2016**, 7849890 (2016).
39. de Sousa, E. M. F. & Vermeulen, L. Wnt signaling in cancer stem cell biology. *Cancers* **8**, 60 (2016).
40. Song, Y., Lee, S., Kim, J. R. & Jho, E. H. Pja2 inhibits Wnt/beta-catenin signaling by reducing the level of TCF/LEF1. *Int. J. Stem Cells* **11**, 242–247 (2018).
41. Chen, Z., Wei, X., Shen, L., Zhu, H. & Zheng, X. 20(S)-ginsenoside-Rg3 reverses temozolomide resistance and restrains epithelial-mesenchymal transition progression in glioblastoma. *Cancer Sci.* **110**, 389–400 (2019).
42. Turgeon, M. O., Perry, N. J. S. & Poulogiannis, G. DNA damage, repair, and cancer metabolism. *Front. Oncol.* **8**, 15 (2018).
43. Lee, D. et al. Folate cycle enzyme MTHFD1L confers metabolic advantages in hepatocellular carcinoma. *J. Clin. Invest.* **127**, 1856–1872 (2017).
44. Rocha, C. R., Kajitani, G. S., Quinet, A., Fortunato, R. S. & Menck, C. F. NRF2 and glutathione are key resistance mediators to temozolomide in glioma and melanoma cells. *Oncotarget* **7**, 48081–48092 (2016).
45. Rubenstein, M. et al. In vivo establishment of T98G human glioblastoma. *Methods Find Exp. Clin. Pharmacol.* **21**, 391–393 (1999).
46. Lenting, K., Verhaak, R., Ter Laan, M., Wesseling, P. & Leenders, W. Glioma: experimental models and reality. *Acta Neuropathol.* **133**, 263–282 (2017).

## ACKNOWLEDGEMENTS

We thank Dr. Michael E. Pacold (Grossman School of Medicine, New York University) and Prof. David M. Sabatini (Massachusetts Institute of Technology) for their kind sharing of the detailed protocol for in vivo administration of NCT503.

## AUTHOR CONTRIBUTIONS

All authors made substantial contributions to this study. Lei Jin was responsible for conceptualization, study design, investigation, acquisition, analysis and interpretation of data and original manuscript drafting. Karrie Mei-Yee Kiang and Stephen Yin Cheng were responsible for conceptualization and review of the manuscript. Gilberto Ka-Kit Leung was responsible for supervision, conceptualization and revision of manuscript and gave final approval of submission and publication.

## COMPETING INTERESTS

The authors declare no competing interests.

## ETHICS APPROVAL AND CONSENT TO PARTICIPATE

The research committee of the University of Hong Kong has reviewed and approved the study according to the principles expressed in the Declaration of Helsinki.

## ADDITIONAL INFORMATION

**Supplementary information** The online version contains supplementary material available at https://doi.org/10.1038/s41374-021-00666-7.

**Correspondence** and requests for materials should be addressed to Gilberto Ka-Kit Leung.

**Reprints and permission information** is available at http://www.nature.com/reprints

**Publisher's note** Springer Nature remains neutral with regard to jurisdictional claims in published maps and institutional affiliations.